

AD-A068 166

WASHINGTON UNIV SEATTLE DEPT OF MECHANICAL ENGINEERING F/G 20/11
INFLUENCE OF DYNAMIC FRACTURE TOUGHNESS ON DYNAMIC CRACK PROPAG--ETC(U)
MAR 78 L HODULAK, A S KOBAYASHI, A F EMERY N00014-76-C-0060

UNCLASSIFIED

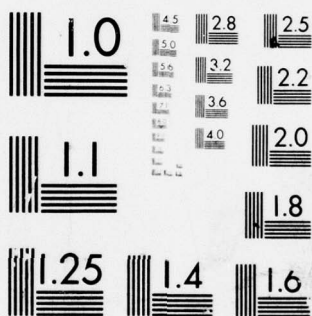
TR-36

NL

|OF|

AD
A068166





MICROCOPY RESOLUTION TEST CHART
NATIONAL BUREAU OF STANDARDS-1963-A

AD A068166

DDC FILE COPY

LEVEL

12

Office of Naval Research

Contract N00014-76-C-0060 NR 064-478

Technical Report No. 36

INFLUENCE OF DYNAMIC FRACTURE TOUGHNESS
ON DYNAMIC CRACK PROPAGATION

by
L. Hodulak, A.S. Kobayashi and A.F. Emery

March 1978

DDC
MAY 2 1979

The research reported in this technical report was made possible through support extended to the Department of Mechanical Engineering, University of Washington, by the Office of Naval Research under Contract N00014-76-C-0060, NR 064-478. Reproduction in whole or in part is permitted for any purpose of the United States Government.

Department of Mechanical Engineering
College of Engineering
University of Washington

This document has been approved
for public release and sale; its
distribution is unlimited.

440344

79 05 01 012

ACCESSION	NTIS	Section	<input checked="" type="checkbox"/>
NTIS	NTIS	Section	<input type="checkbox"/>
NTIS	NTIS	Section	<input type="checkbox"/>
DISTANCE FROM THE POINT OF			
P. 0.00			
A			

INFLUENCE OF DYNAMIC FRACTURE TOUGHNESS ON DYNAMIC CRACK PROPAGATION

by

L. Hodulak, A.S. Kobayashi and A.F. Emery

University of Washington

Department of Mechanical Engineering

Seattle, Washington 98195

ABSTRACT

A dynamic finite element code was used in its "propagation mode" to assess the differences in dynamic crack propagation in a wedge-loaded (WL) single-edged notch (SEN) specimen, a tapered double cantilever beam (TDCB) specimen and a rectangular double cantilever beam (RDCB) specimen. The dynamic fracture toughness, K_{ID} , versus the crack velocity, \dot{a} , relations determined experimentally for WL-SEN, WL-TDCB and WL-RDCB specimens machined from Araldite B were used as dynamic fracture criteria and the resultant K_{ID} variations with crack propagations in the three specimens were compared with the corresponding experimental results. While the specific K_{ID} versus \dot{a} relations established for each specimen obviously yielded calculated K_{ID} which were in best agreement with the experimental K_{ID} for the respective specimen, the K_{ID} versus \dot{a} relation for the large WL-SEN specimen provided the best overall fit between the calculated and measured K_{ID} variations with crack propagation in all three specimens.

INTRODUCTION

During the past several years, dynamic photoelasticity [1-3] and dynamic caustic [4,5] have been used in an attempt to identify a fundamental law which governs dynamic crack propagation in solids. These optical techniques provide the near-field, dynamic state of stress surrounding a running crack and thus offer means of extracting the dynamic stress intensity factor associated with this stress field. Although most of these investigations have been confined to the studies of dynamic responses in polymers, birefringent coating technique [6] and reflection caustic [5] are being used to extend these optical techniques for studying dynamic fracture of metals. All investigations using these optical techniques, however, have been confined to the dynamic analyses of fracture specimens of specific geometries. It is interesting to note that the University of Maryland (UM) [1,2] group chose relatively large Homalite-100 fracture specimens in comparison to the smaller Homalite-100 specimens used at the University of Washington (UW) [3] and the group at the Institut für Festkörpermechanik (IFKM) [4, 5] used medium and small size Araldite B specimens. The resultant dynamic stress fracture toughness, K_{ID} , versus crack velocity relation, \dot{a} , obtained by the UM group showed that the K_{ID} versus \dot{a} relation for Homalite-100 to be essentially independent of specimen configurations. The UW and IFKM results in Homalite-100 and Araldite B, respectively, on the other hand, showed K_{ID} versus \dot{a} relation to be somewhat dependent on specimen geometry.

These differences, which admittedly are not excessive, in K_{ID} versus \dot{a} relations pose a fundamental question as to whether dynamic crack propagation is solely governed by the current state of crack tip stresses, which are characterized by the dynamic fracture toughness of K_{ID} , or whether it should

79 05 01 012

carry the influence of past propagation history such as the rate of change of dynamic fracture toughness, \dot{K}_{ID} . The latter obviously would not allow K_{ID} versus \dot{a} to be a unique material property. In spite of this controversy, past numerical analysis [7] has indicated that perhaps variations in the K_{ID} versus \dot{a} relation do not substantially affect the total dynamic motion leading the authors to question the sensitivity of the calculated dynamic crack propagation to the specific K_{ID} versus \dot{a} relation used.

The authors thus undertook a sensitivity study using the IFKM test results which included smaller fracture specimens machined from previously fractured larger specimens and which reduced the material variability in establishing K_{ID} versus \dot{a} relations for the various fracture specimens. In the following some of the salient features of this study are reported.

DYNAMIC FRACTURE ANALYSIS

The recent revisions made in the authors' previously updated dynamic finite element code [8] are discussed in detail in Reference [9]. Briefly, the most recent improvements include a better controlled numerical algorithm prescribing nodal force at the crack tip node during crack extension in the explicit dynamic finite element code of HONDO [10]. Fracture energy was computed from the dissipated energy using the force and displacement at the nodal point being released. The dynamic stress intensity factor was then computed from the fracture energy using Freund's relation [11]. The improved dynamic fracture mechanics code was first used in its "propagation" and then in its "generation" modes, as designated by Kanninen [12], of crack propagation in order to verify the internal consistency of the total fracture mechanics package.

The improved code was then used both in its propagation and generation modes to analyze two fracturing wedge-loaded, rectangular double cantilever beam (WL-RDCB) specimen tested by Kalthoff et al. [13]. Negligible differences between the two numerical K_{ID} throughout the fracture process obtained through the propagation and generation modes proved the sought internal consistency of the code. Good agreement between the numerically and experimentally determined K_{ID} further showed the validity of the dynamic fracture model used. It was also shown that when the generation mode is used in conjunction with the measured crack position versus time data, experimental errors in the latter could grossly distort the computed K_{ID} values. The inevitable limitation in crack position measurements was overcome by using the smoothed crack position versus time as well as an associated smoothed crack velocity relation as input data in the generation calculations.

The above studies also showed that the propagation calculation resulted in less oscillations in the calculated K_{ID} but the calculated and measured crack lengths at crack arrest were not always in complete agreement. This sensitivity of the arrest crack length to input K_{ID} versus \dot{a} relation in the propagation calculation made it ideal for the sensitivity study reported in this paper.

FRACTURE SPECIMENS AND MATERIAL DATA

The three specimens which were analyzed by the dynamic finite element code are the wedge-loaded (WL) single-edge notched (SEN) specimen, rectangular double cantilever beam (RDCB) specimen and tapered double cantilever beam (TDCB) specimen which were machined from a 10 mm thick Araldite B and analyzed with dynamic caustics by Kalthoff et al. [4,5]. The specimen geometries are given in Figure 1 and a typical finite element breakdown of the WL-SEN specimen is given in Figure 2. The finite element breakdown used for the WL-RDCB and

WL-TDCB specimens are similar to those used in Reference [9] with an obvious reduction in scale.

Extensive experimental investigation by Hahn et al. [7] has shown that the wedge-loaded pins could leave the wedge and travel outwards in the steel specimens. When such pin motion is accounted for in K_{ID} computation, an attendant increase in the K_{ID} during crack propagation was observed [14]. The additional input energy due to any possible separation of the steel loading pins from the steel wedge should be considerably smaller due to the smaller mass density and the two orders of magnitude larger compliance of the Araldite B specimens in comparison to the steel specimen studied in Reference [14]. Thus the possible loading pin motion was ignored and constant displacements were prescribed at the pin holes in the dynamic finite element analysis.

Material constants of Araldite B used for this analysis are modulus of elasticity $E = 3.38$ GPa, Poisson ratio of $\nu = 0.33$ and mass density, $\rho = 1047$ kg/m³. Dynamic fracture toughness K_{ID} , versus crack velocity, \dot{a} , relations shown in Figure 3, are based on the experimental data from Ref. [15].

Since the dynamic crack initiation stress intensity factors, K_{IQ} , were not reported in Reference [15] for any of the three specimens, K_{IQ} s were either back-calculated by static analysis using the estimated mean values of oscillating K_{ID} values for the WL-RDCB and WL-TDCB specimens or estimated for the WL-SEN specimen. Given the K_{IQ} value and one of the three K_{ID} versus \dot{a} relations, the crack was propagated dynamically in the WL-SEN, WL-TDCB and WL-RDCB specimens using the improved fracture dynamic code.

RESULTS

WL-SEN Specimen

The first numerical analysis involved a propagation analysis of the WL-SEN specimen of Figure 1 using three K_{ID} versus \dot{a} relations of Figure 3 and a $K_{IQ} = 1.08 \text{ MPa } \sqrt{\text{m}}$. The resultant K_{ID} crack tip motion of this propagation calculation are shown in Figures 4 and 5, respectively. Significant differences are noted especially in the second two thirds of crack propagation prior to crack arrest, where the two curves obtained by using the K_{ID} versus \dot{a} relations for the WL-TDCB and WL-RDCB specimens grossly underestimate by more than a factor of two the total jump distance at crack arrest.

Figure 5 shows that the computed crack propagation time using the K_{ID} versus \dot{a} relation is about one half and two thirds, respectively, of the actual propagation time. The underestimation in computed crack arrest length and time using the K_{ID} versus \dot{a} relations of the WL-TDCB and WL-RDCB is due to the fact that the propagation calculation is terminated when the computed dynamic stress intensity factor falls below the minimum K_{ID} values in Figure 3 thus indicating the extreme sensitivity of these values to the seemingly small shifts in the minimum K_{ID} .

WL-TDCB Specimen

Figure 6 shows the K_{ID} as a function of \dot{a} of a WL-TDCB specimen again using the three K_{ID} versus \dot{a} relations of Figure 3 and $K_{IQ} = 2.08 \text{ MPa } \sqrt{\text{m}}$. The pronounced second maximum in K_{ID} seen in the WL-SEN specimen as well as in the previously analyzed large WL-RDCB specimen [9], is considerably smaller in the current WL-TDCB specimen. The computed jump distances at crack arrest obtained by the use of the three K_{ID} versus \dot{a} relations are in reasonable agreement with experimental results. Although not obvious from Figure 6,

the computed K_{ID} increased again after the initial crack arrest to a value approaching the measured K_{ID} at crack arrest if a slow crack propagation was prescribed just after the arrest.

Figure 7 shows the K_{ID} versus time relation for a WL-TDCB specimen using the three K_{ID} versus \dot{a} relations. Although the three calculated K_{ID} are in excellent agreement with each other, the calculated crack arrest times are considerably smaller than that found experimentally.

Figure 8 shows the computed K_{ID} for a WL-RDCB specimen using the three K_{ID} versus \dot{a} relations and a $K_{IQ} = 2.0 \text{ MPa } \sqrt{\text{m}}$. Note that the crack length at crack arrest obtained by using the K_{ID} versus \dot{a} relations for large WL-SEN and small WL-TDCB specimens are approximately 5% larger and smaller, respectively, than the measured crack length at crack arrest. Interestingly enough, all the three calculations underpredict the time to crack arrest as shown by Figure 9.

CONCLUSIONS

Propagation studies of three Araldite B dynamic fracture specimens, i.e. WL-SEN, WL-TDCB and WL-RDCB, using the individually generated K_{ID} versus \dot{a} relations showed that best agreement between calculated and measured K_{ID} values can be obtained, as expected when the respective K_{ID} versus \dot{a} relation is used in analyzing each specimen.

Calculated crack arrest length and crack arrest time for a WL-SEN specimen with small variations in K_{ID} are sensitive to the slight shift in the minimum dynamic stress intensity factor, K_{Im} , in the K_{ID} versus \dot{a} relation.

In this study conservative estimates of the crack arrest lengths in the small specimens, i.e. WL-TDCB and WL-RDCB can be obtained by using the K_{ID} versus \dot{a} relation with the smallest K_{Im} , i.e. the relation generated by the larger WL-SEN specimen.

DISCUSSIONS

Although only three dynamic fracture specimens were studied in this paper, this comparative study indicates that the specimen dependent K_{ID} versus \dot{a} relation advocated by some [3,4,5] is valid. If such is the case, the results also imply that dynamic propagation of a crack is not controlled solely by the instantaneous dynamic state surrounding a running crack and that further fundamental investigation on the law(s) governing dynamic crack propagation is necessary. Crack propagation in the presence of severe dynamic loadings, such as impact loading of a small fracture specimen [6,7] could accentuate such dynamic conditions and thus warrants further investigation.

In the interim, however, conservative estimates of the dynamic crack propagation response and the crack length at crack arrest can be made by using the minimum K_{ID} at the knee and a maximum K_{ID} at the shelf of a K_{ID} versus \dot{a} relation which in this study happens to be that established for large WL-SEN.

ACKNOWLEDGEMENTS

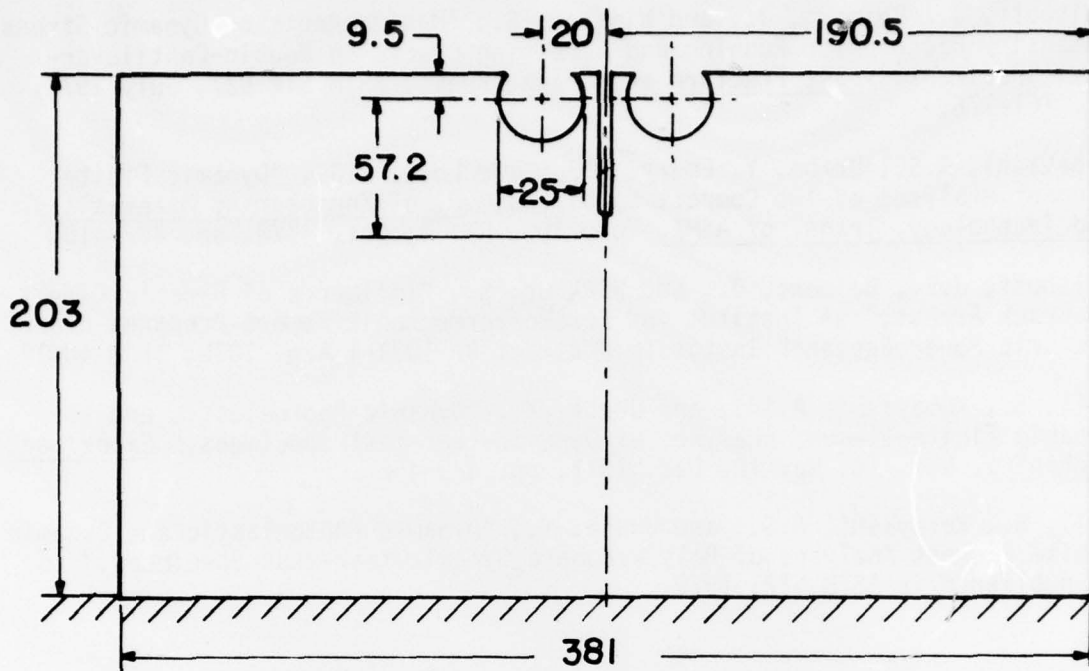
The results of this investigation were obtained in a research contract funded by the Office of Naval Research under Contract N00014-76-C-0060 NR 064-478. The authors wish to acknowledge the support and encouragement of Dr. N.R. Perrone of ONR during the course of this investigation. The first author, L. Hodulak, was supported by a postdoctoral fellowship from the Deutsche Forschungsgemeinschaft, FRG. The authors also wish to acknowledge the discussions with Dr. J. F. Kalthoff. Institut für Festkörpermechanik.

REFERENCES

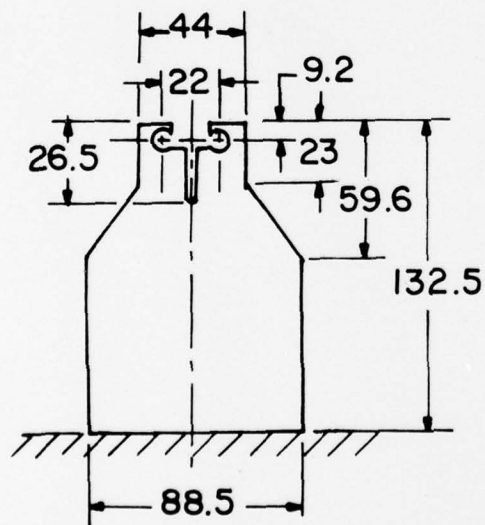
1. Kobayashi, T. and Dally, J.W., "The Relation Between Crack Velocity and Stress Intensity Factor in Birefringent Polymers," Fast Fracture and Crack Arrest, ASTM STP 627, 1977, pp. 257-273.
2. Irwin, G.R., Dally, J.W., Kobayashi, T., Fourney, W.L., and Etheridge, J.M., "Photoelastic Studies of Crack Propagation and Crack Arrest," a University of Maryland report prepared under U.S. Nuclear Regulatory Commission Contract AT(49-24)-0172, Sept. 1977.
3. Kobayashi, A.S. and Mall, S., "Dynamic Fracture Toughness of Homalite-100," Experimental Mechanics, Vol. 18, No. 1, Jan. 1978, pp. 11-18.
4. Kalthoff, J., "Effect of Specimen Geometry on Crack Arrest Toughness," a paper presented at the Joint ASME/CSME Pressure Vessel and Piping Conf., Montreal, Canada, June 25-30, 1979.
5. Kalthoff, J., Beinert, J., and Winkler, S., "Experimental Analysis of Dynamic Effects in Different Crack Arrest Specimens," a paper presented at the ASTM E-24 Symposium on Crack Arrest Methodology and Applications, Philadelphia, Nov. 6-7, 1978.
6. Kobayashi, T. and Dally, J.W., "Dynamic Photoelastic Characterization of Instantaneous Stress Intensity Factor for 4340 Alloy Steel," *ibid loc. cit.*
7. Hahn, G.T., Gehlen, P.C., Hoagland, R.G., Marshall, C.W., Kanninen, M.F., Popelar, C., and Rosenfield, A.R., "Critical Experiments, Measurements and Analyses to Establish a Crack Arrest Methodology for Nuclear Pressure Vessel Steels," a Battelle Columbus Laboratories report prepared under U.S. Nuclear Regulatory Commission Contract No. W-7405-Ing-92, Oct. 1976, BMI-NUREG-1959.
8. Kobayashi, A.S., Mall, S., Urabe, Y., and Emery, A.F., "A Numerical Dynamic Fracture Analysis of Three Wedge-Loaded DCB Specimens," Numerical Methods in Fracture Mechanics, edited by A.R. Luxmoore and D.R.J. Owens, University College of Swansea, Jan. 9-13, 1978, pp. 673-684.
9. Hodulak, L., Kobayashi, A.S., and Emery, A.F., "A Critical Examination of a Numerical Fracture Dynamic Code," a paper submitted for presentation at the 12th ASTM Annual Symposium on Fracture Mechanics, Washington University, May 20-23, 1979.
10. Key, S.W., "HONDO, A Finite Element Computer Program for the Large Deformation Responses of Axisymmetric Solids," Sandia Laboratories.
11. Freund, L.B., "Crack Propagation in an Elastic Solid Subjected to General Loading-II Non-Uniform Rate of Extension," J. of Mechanics and Physics of Solids, Vol. 20, 1972, pp. 141-152.
12. Kanninen, M.F., "A Critical Appraisal of Solution Techniques in Dynamic Fracture Mechanics," Numerical Methods in Fracture Mechanics, edited by A.R. Luxmoore and D.R.J. Owens, University College of Swansea, Jan. 1978, pp. 612-633.

13. Kalthoff, J., Beinert, J., and Winkler, S., "Measurements of Dynamic Stress Intensity Factors for Running and Arresting Cracks in Double-Cantilever-Beam Specimens," Fast Fracture and Crack Arrest, ASTM STP 627, July 1977, pp. 161-176.
14. Kobayashi, A.S., Urabe, Y., Emery, A.F., and Love, W.J., "Dynamic Finite Element Analyses of Two Compact Specimens," J. of Engineering Materials and Technology, Trans. of ASME, Vol. 100, No. 4, Oct. 1978, pp. 402-410.
15. Kalthoff, J.F., Beinert, J., and Winkler, S., "Influence of Dynamic Effect on Crack Arrest," an Institut fur Festkorpermechanik report prepared under Electric Power Research Institute Contract RP 1022-1 Aug. 1978, IKFM 40412.
16. Mall, S., Kobayashi, A.S., and Urabe, Y., "Dynamic Photoelastic and Dynamic Finite-element Analyses of Dynamic-tear-test Specimens," Experimental Mechanics, Vol. 18, No. 12, Dec. 1978, pp. 449-456.
17. Mall, S., Kobayashi, A.S., and Urabe, Y., "Dynamic Photoelastic and Dynamic Finite Element Analyses of Polycarbonate Dynamic-tear-test Specimens," to be published in ASTM STP, 1979.

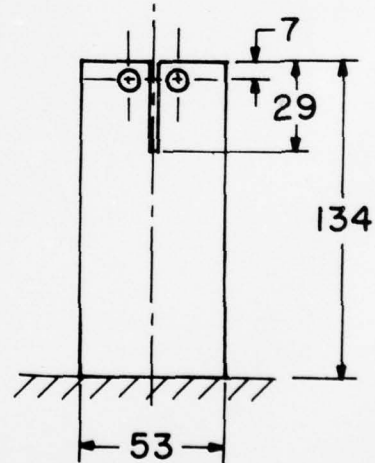
ALL DIMENSIONS IN mm
PLATE THICKNESS 10



WL-SEN SPECIMEN



WL-TDCB SPECIMEN



WL-RDCB SPECIMEN

FIGURE 1. THREE DYNAMIC FRACTURE SPECIMENS:
WEDGE LOADED SINGLE-EDGED NOTCH SPECIMEN (WL-SEN).
WEDGE LOADED TAPERED DOUBLE CANTILEVER BEAM
SPECIMEN (WL-TDCB).
WEDGE LOADED RECTANGULAR DOUBLE CANTILEVER
BEAM SPECIMEN (WL-RDCB).

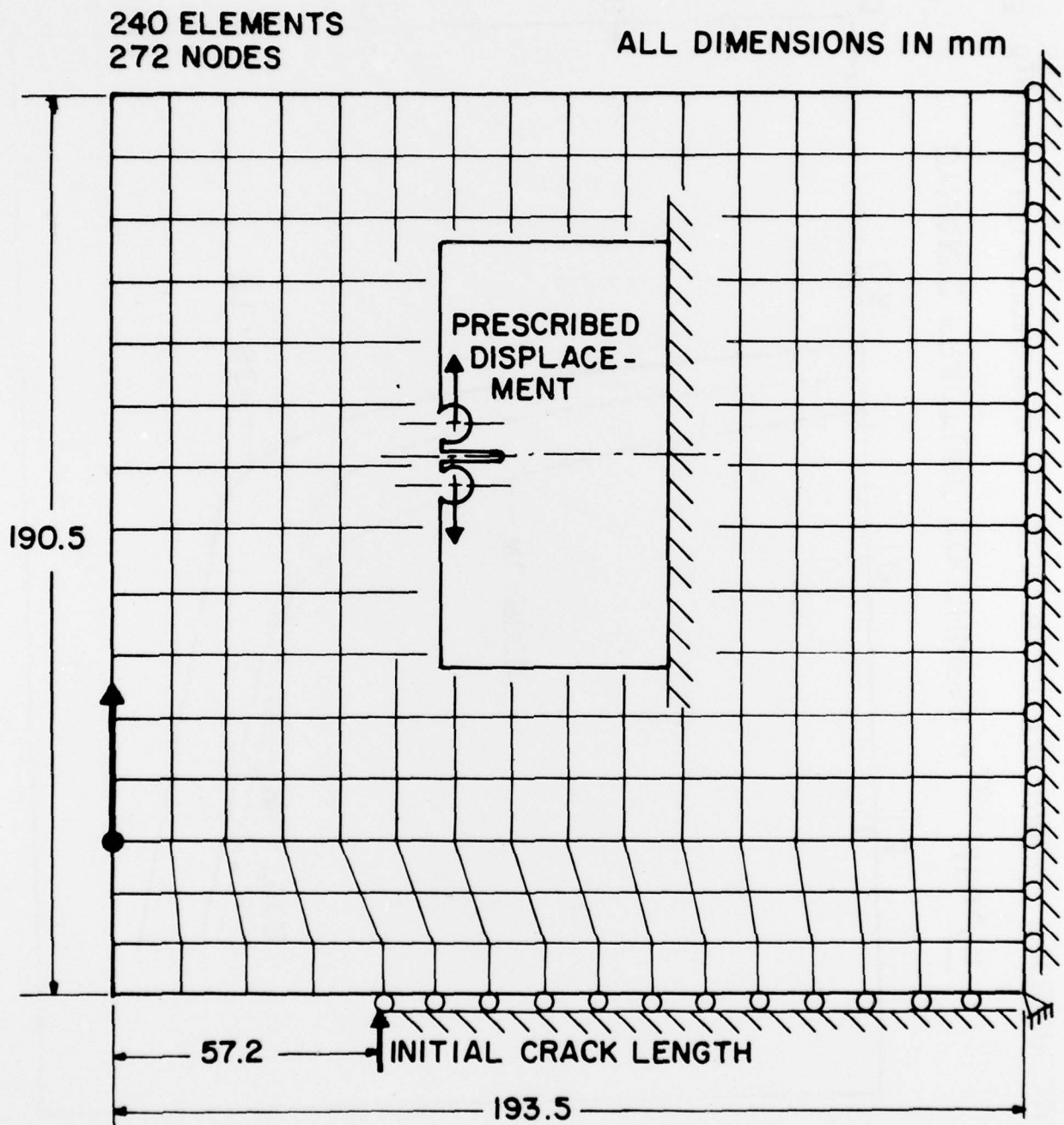


FIGURE 2. FINITE ELEMENT BREAKDOWN OF WL-SEN SPECIMEN.

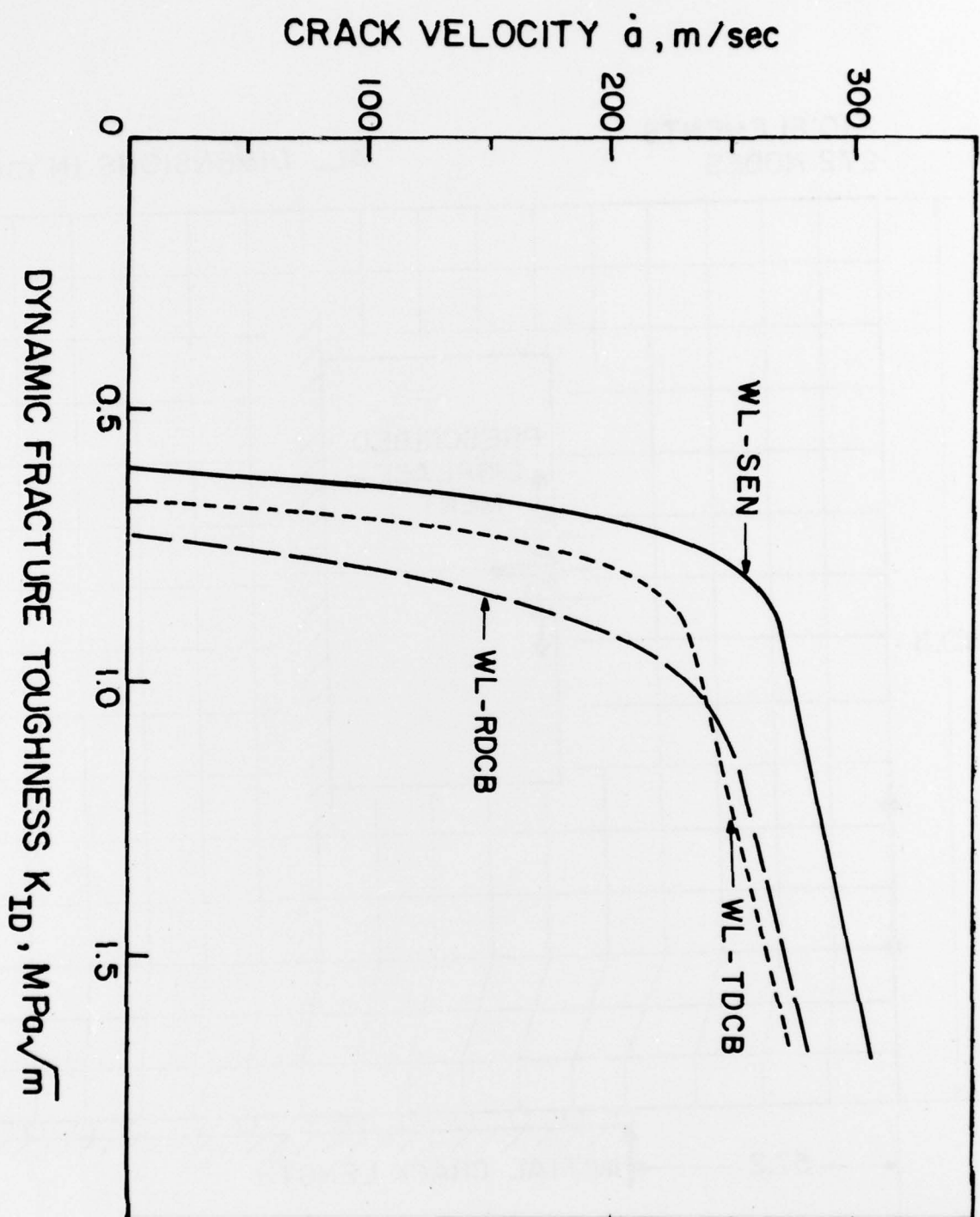


FIGURE 3. K_{ID} vs \dot{a} RELATIONS FOR WL-SEN, WL-TDCB AND WL-RDCB SPECIMENS ARLDITE B.

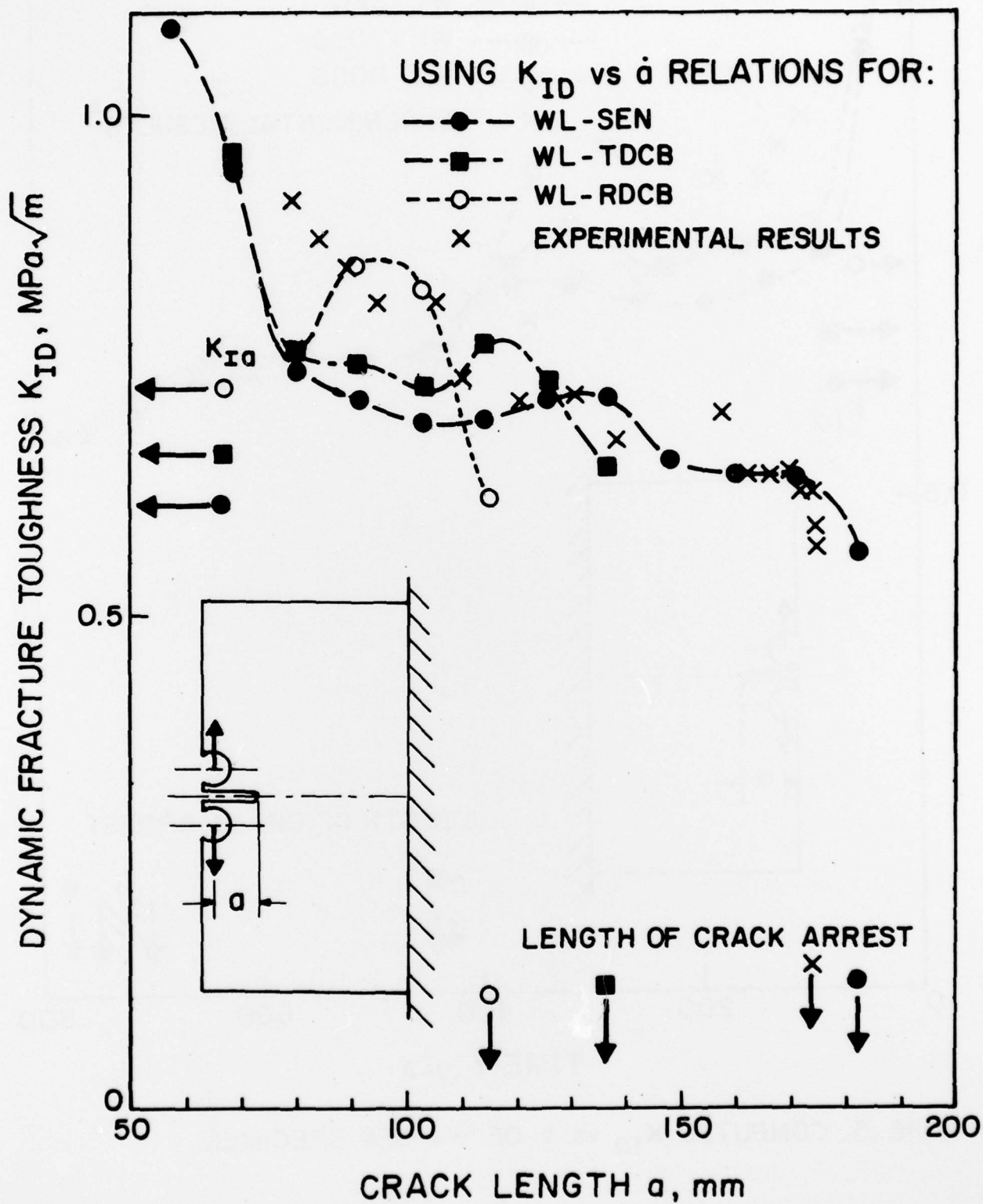


FIGURE 4. COMPUTED K_{ID} vs a OF WL-SEN SPECIMEN.

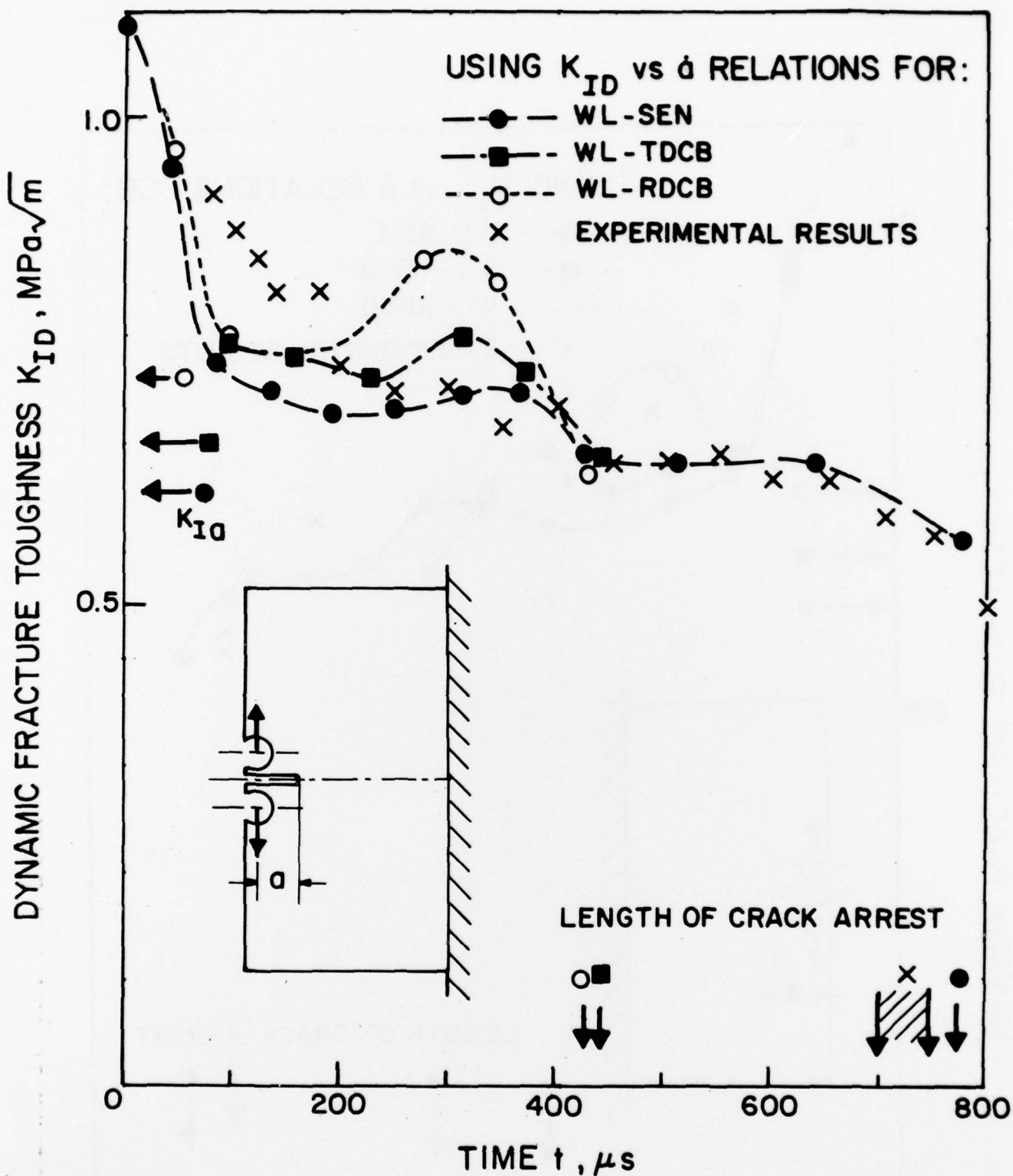


FIGURE 5. COMPUTED K_{ID} vs t OF WL-SEN SPECIMEN.

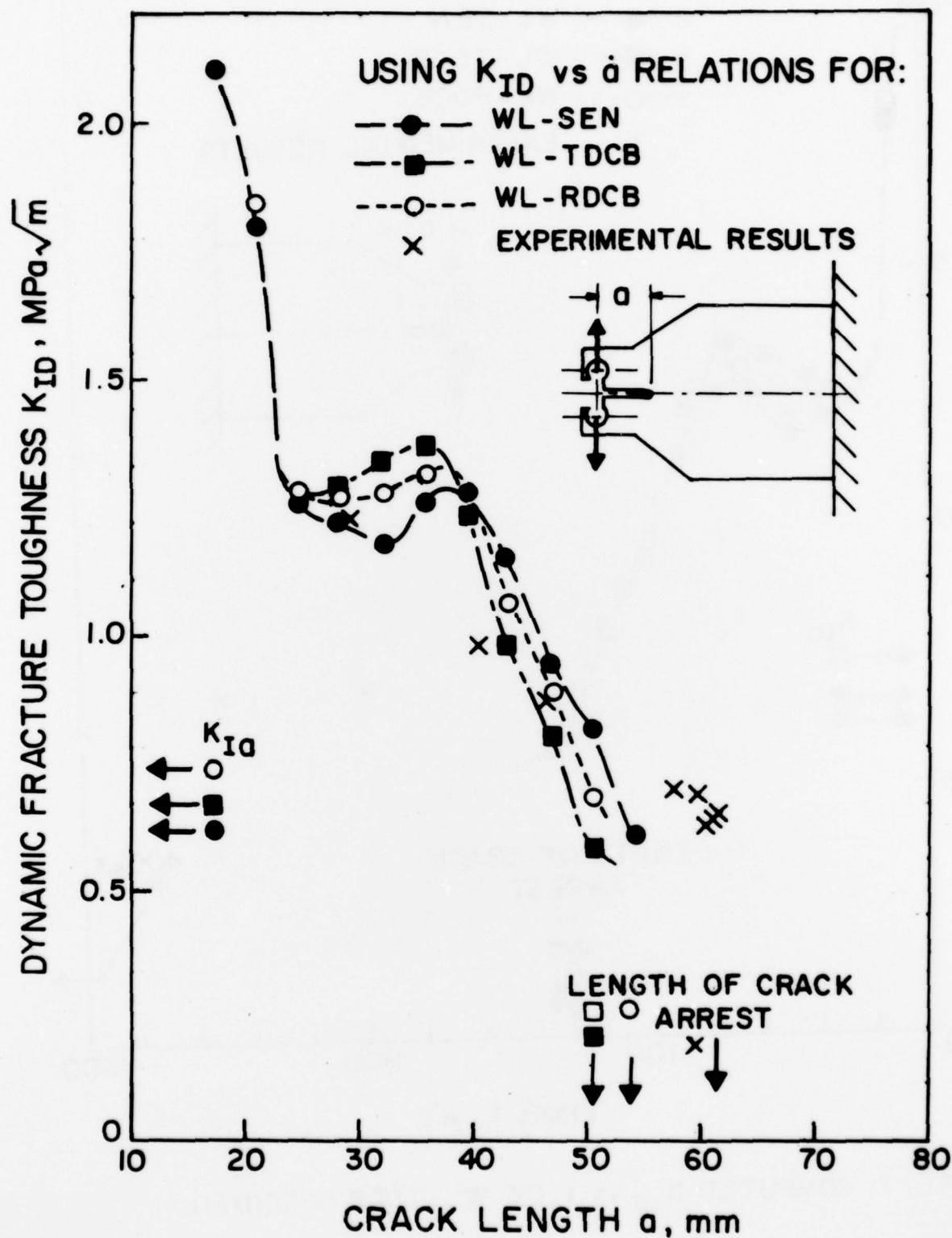


FIGURE 6. COMPUTED K_{ID} vs a OF WL-TDCB SPECIMEN.

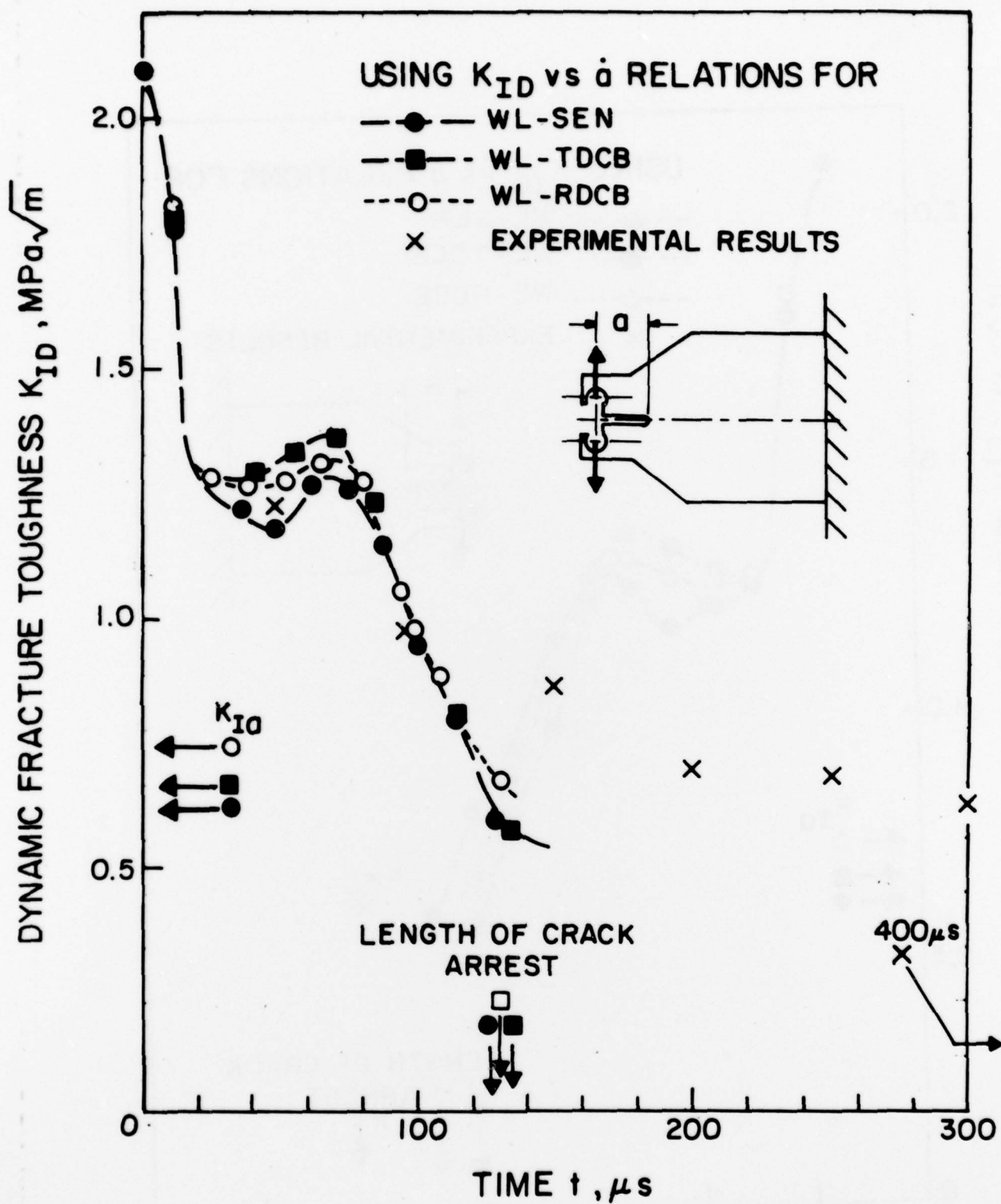


FIGURE 7. COMPUTED K_{ID} vs t OF WL-TDCB SPECIMEN.

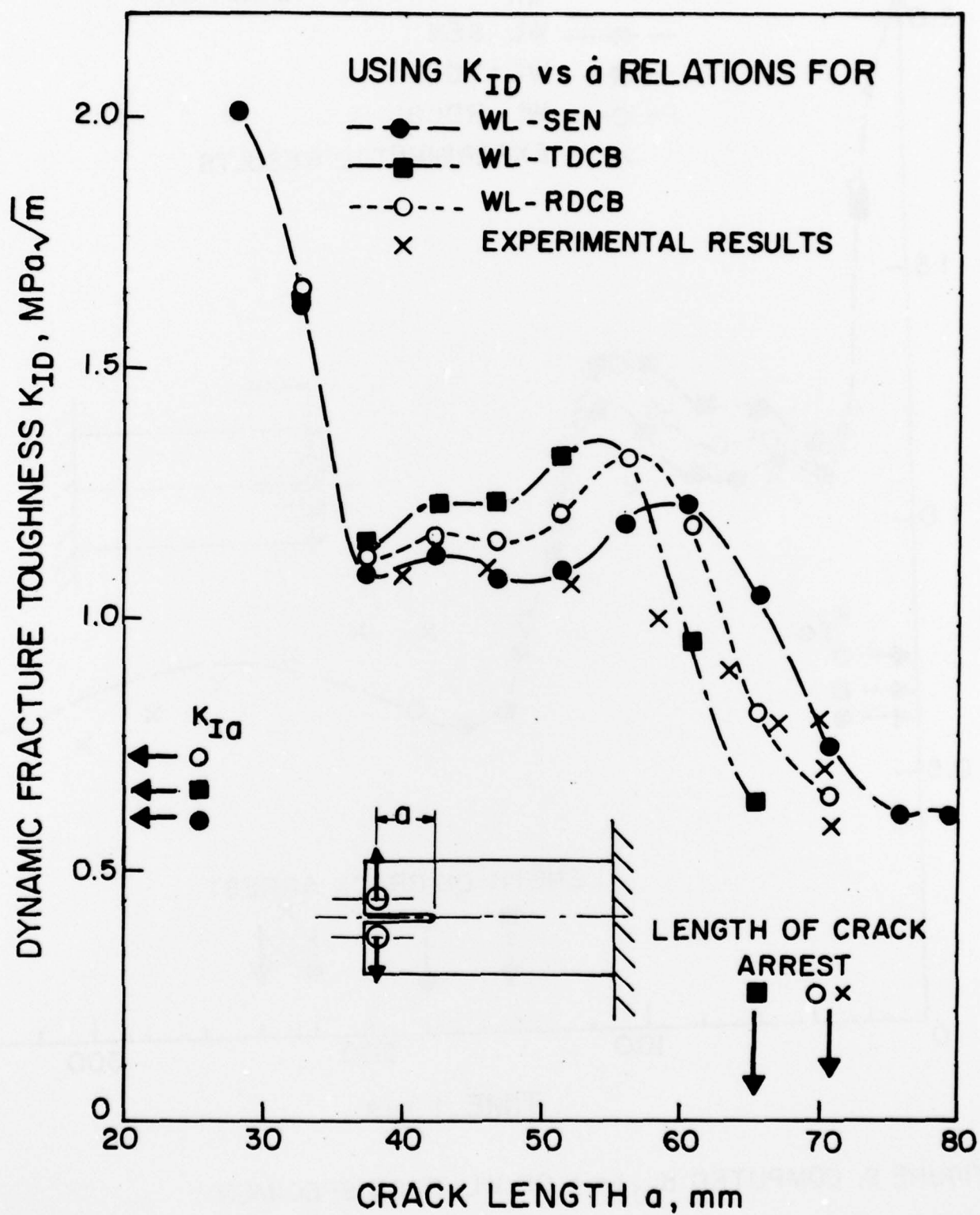


FIGURE 8. COMPUTED K_{ID} vs a OF WL-RDCB SPECIMEN.

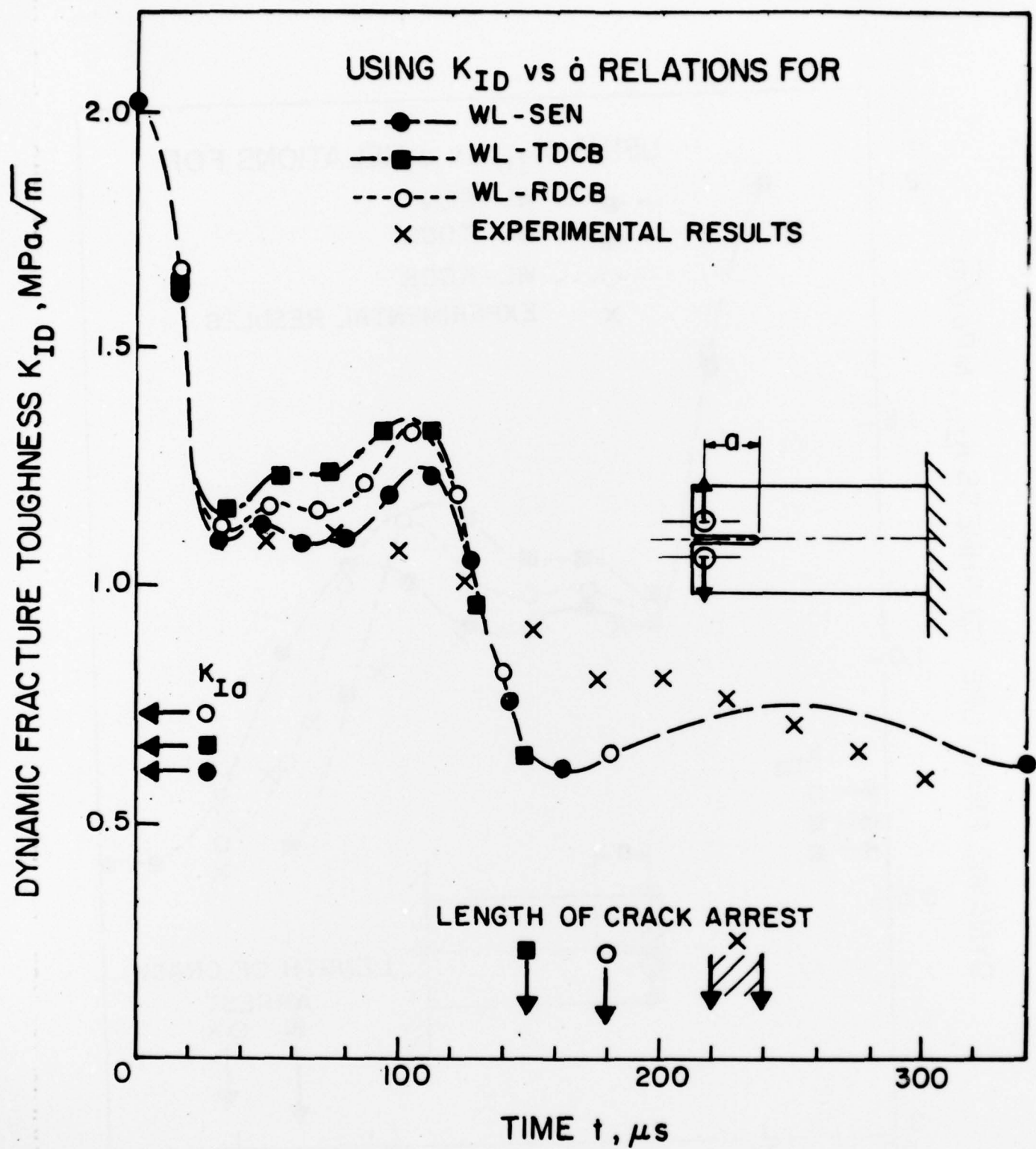


FIGURE 9. COMPUTED K_{ID} vs t OF WL-RDCB SPECIMEN.

PART 1 - Government

Administrative and Liaison Activities

Office of Naval Research
Department of the Navy
Arlington, VA 22217
Attn: Code 474 (2)
Code 471
Code 200

Director
Office of Naval Research
Branch Office
666 Summer Street
Boston, MA 02210

Director
Office of Naval Research
Branch Office
536 South Clark Street
Chicago, IL 60605

Director
Office of Naval Research
New York Area Office
715 Broadway - 5th Floor
New York, NY 10003

Director
Office of Naval Research
Branch Office
1030 East Green Street
Pasadena, CA 91106

Naval Research Laboratory (6)
Code 2627
Washington, DC 20375

Defense Documentation Center (12)
Cameron Station
Alexandria, VA 22314

Navy

Undersea Explosion Research Division
Naval Ship Research and Development
Center
Norfolk Naval Shipyard
Portsmouth, VA 23709
Attn: Dr. E. Palmer, Code 177

Navy (Con't.)

Naval Research Laboratory
Washington, DC 20375
Attn: Code 8400
8410
8430
8440
6300
6390
6380

David W. Taylor Naval Ship Research
and Development Center
Annapolis, MD 21402
Attn: Code 2740
28
281

U.S. Naval Weapons Center
China Lake, CA 93555
Attn: Code 4062
4520

Commanding Officer
U.S. Naval Civil Engineering Laboratory
Code L31
Port Hueneme, CA 93041

Naval Surface Weapons Center
White Oak
Silver Spring, MD 20910
Attn: Code R-10
G-402
K-82

Technical Director
Naval Ocean Systems Center
San Diego, CA 92152

Supervisor of Shipbuilding
U.S. Navy
Newport News, VA 23607

U.S. Navy Underwater Sound
Reference Division
Naval Research Laboratory
P.O. Box 8337
Orlando, FL 32806

Navy (Con't.)

Chief of Naval Operations
Department of the Navy
Washington, DC 20350
Attn: Code OP-098

Strategic Systems Project Office
Department of the Navy
Washington, DC 20376
Attn: NSP-200

Naval Air Systems Command
Department of the Navy
Washington, DC 20361
Attn: Code 5302 (Aerospace and Structures)
604 (Technical Library)
320B (Structures)

Naval Air Development Center
Director, Aerospace Mechanics
Warminster, PA 18974

U.S. Naval Academy
Engineering Department
Annapolis, MD 21402

Naval Facilities Engineering Command
200 Stovall Street
Alexandria, VA 22332

Attn: Code 03 (Research and Development)
04B
04S
14114 (Technical Library)

Naval Sea Systems Command
Department of the Navy
Washington, DC 20362
Attn: Code 03 (Research and Technology)
037 (Ship Silencing Division)
035 (Mechanics and Materials)

Naval Ship Engineering Center
Department of the Navy
Washington, DC 20362
Attn: Code 6105G
6114
6120D
612B
6129

Commanding Officer and Director
David W. Taylor Naval Ship
Research and Development Center
Bethesda, MD 20084
Attn: Code 042

17
172
173
174
1800
1844
1102.1
1900
1901
1945
1960
1962

Naval Underwater Systems Center
Newport, RI 02840
Attn: Dr. R. Trainor

Naval Surface Weapons Center
Dahlgren Laboratory
Dahlgren, VA 22448
Attn: Code 604
G20

Technical Director
Mare Island Naval Shipyard
Vallejo, CA 94592

U.S. Naval Postgraduate School
Library
Code 0384
Monterey, CA 93940

Webb Institute of Naval Architecture
Attn: Librarian
Crescent Beach Road, Glen Cove
Long Island, NY 11542

Army

Commanding Officer (2)
U.S. Army Research Office
P.O. Box 12211
Research Triangle Park, NC 27709
Attn: Mr. J. J. Murray,
CRD-AA-1P

Watervliet Arsenal
MAGGS Research Center
Watervliet, NY 12189
Attn: Director of Research

U.S. Army Materials and Mechanics
Research Center
Watertown, MA 02172
Attn: Dr. R. Shea, DRXMR-T

U.S. Army Missile Research and
Development Center
Redstone Scientific Information
Center
Chief, Document Section
Redstone Arsenal, AL 35809

Army Research and Development
Center
Fort Belvoir, VA 22060

NASA

National Aeronautics and Space Administration
Structures Research Division
Langley Research Center
Langley Station
Hampton, VA 23365

National Aeronautics and Space Administration
Associate Administrator for Advanced
Research and Technology
Washington, DC 20546

Scientific and Technical Information Facility
NASA Representative (S-AK/DL)
P.O. Box 5700
Bethesda, MD 20014

Air Force

Commander WADD
Wright-Patterson Air Force Base
Dayton, OH 45433
Attn: Code WWRMDD
AFFDL (FDDOS)
Structures Division
AFLC (MCEEA)

Chief Applied Mechanics Group
U.S. Air Force Institute of Technology
Wright-Patterson Air Force Base
Dayton, OH 45433

Chief, Civil Engineering Branch
WLRC, Research Division
Air Force Weapons Laboratory
Kirtland Air Force Base
Albuquerque, NM 87117

Air Force Office of Scientific Research
Bolling Air Force Base
Washington, DC 20332
Attn: Mechanics Division

Department of the Air Force
Air University Library
Maxwell Air Force Base
Montgomery, AL 36112

Other Government Activities

Commandant
Chief, Testing and Development Division
U.S. Coast Guard
1300 E Street, NW
Washington, DC 20226

Technical Director
Marine Corps Development
and Education Command
Quantico, VA 22134
Director Defense Research
and Engineering
Technical Library
Room 3C128
The Pentagon
Washington, DC 20301

Director
National Bureau of Standards
Washington, DC 20034
Attn: Mr. B. L. Wilson, EM 219

Dr. M. Gaus
National Science Foundation
Environmental Research Division
Washington, DC 20550

Library of Congress
Science and Technology Division
Washington, DC 20540

Director
Defense Nuclear Agency
Washington, DC 20305
Attn: SPSS

Mr. Jerome Persh
Staff Specialist for Materials
and Structures
OUSDRAE, The Pentagon
Room 3D10B9
Washington, DC 20301

Chief, Airframe and Equipment Branch
FS-120
Office of Flight Standards
Federal Aviation Agency
Washington, DC 20553

National Academy of Sciences
National Research Council
Ship Hull Research Committee
2101 Constitution Avenue
Washington, DC 20418
Attn: Mr. A. R. Lytle

National Science Foundation
Engineering Mechanics Section
Division of Engineering
Washington, DC 20550

Piscataway Arsenal
Plastics Technical Evaluation Center
Attn: Technical Information Section
Dover, NJ 07801

Maritime Administration
Office of Maritime Technology
14th and Constitution Ave., NW
Washington, DC 20230

Maritime Administration
Office of Ship Construction
14th and Constitution Ave., NW
Washington, DC 20230

PART 2 - Contractors and Other Technical Collaborators

Universities

Dr. J. Hensley Oden
University of Texas at Austin
345 Engineering Science Building
Austin, TX 78712

Professor Julius Miklowitz
California Institute of Technology
Division of Engineering
and Applied Sciences
Pasadena, CA 91109

Dr. Harold Liebowitz, Dean
School of Engineering and
Applied Science
George Washington University

Professor Eli Sternberg
California Institute of Technology
Division of Engineering and
Applied Sciences
Pasadena, CA 91109

Professor Paul M. Naught
University of California
Department of Mechanical Engineering
Berkeley, CA 94720

Professor A. J. Durelli
Oakland University
School of Engineering
Rochester, MI 48063

Professor F. L. DiMaggio
Columbia University
Department of Civil Engineering
New York, NY 10027

Professor Norman Jones
Massachusetts Institute of Technology
Department of Ocean Engineering
Cambridge, MA 02139

Professor E. J. Skudrzyk
Pennsylvania State University
Applied Research Laboratory
Department of Physics
State College, PA 16801

Professor J. Kempner
Polytechnic Institute of New York
Department of Aerospace Engineering and
Applied Mechanics
333 Jay Street
Brooklyn, NY 11201

Professor J. Klosner
Polytechnic Institute of New York
Department of Aerospace Engineering and
Applied Mechanics
333 Jay Street
Brooklyn, NY 11201

Professor R. A. Schapery
Texas A&M University
Department of Civil Engineering
College Station, TX 77843

Professor Walter D. Pilkey
University of Virginia
Research Laboratories for the
Engineering Sciences
School of Engineering and
Applied Sciences
Charlottesville, VA 22901

Professor K. D. Willmert
Clarkson College of Technology
Department of Mechanical Engineering
Potsdam, NY 13676

Dr. Walter E. Haistler
Texas A&M University
Aerospace Engineering Department
College Station, TX 77843

Dr. Hussein A. Kamei
University of Arizona
Department of Aerospace and
Mechanical Engineering
Tucson, AZ 85721

Dr. S. J. Fenves
Carnegie-Mellon University
Department of Civil Engineering
Schenley Park
Pittsburgh, PA 15213

Universities (Con't.)

Professor H. W. Liu
Syracuse University
Department of Chemical Engineering
and Metallurgy
Syracuse, NY 13210

Professor S. Bodner
Technion R&D Foundation
Haifa, Israel

Professor Werner Goldsmith
University of California
Department of Mechanical Engineering
Berkeley, CA 94720

Professor R. S. Rivlin
Lehigh University
Center for the Application
of Mathematics
Bethlehem, PA 18015

Professor F. A. Cozzarelli
State University of New York at Buffalo
Division of Interdisciplinary Studies
Karr Parker Engineering Building
Chemistry Road
Buffalo, NY 14214

Professor Joseph L. Rose
Drexel University
Department of Mechanical Engineering
and Mechanics
Philadelphia, PA 19104

Professor B. K. Donaldson
University of Maryland
Aerospace Engineering Department
College Park, MD 20742

Professor Joseph A. Clark
Catholic University of America
Department of Mechanical Engineering
Washington, DC 20064

Professor T. C. Huang
University of Wisconsin-Madison
Department of Engineering Mechanics
Madison, WI 53706

Dr. Samuel B. Batdorf
University of California
School of Engineering
and Applied Science
Los Angeles, CA 90024

Professor Isaac Fried
Boston University
Department of Mathematics
Boston, MA 02215

Professor Michael Pappas
New Jersey Institute of Technology
Newark College of Engineering
323 High Street
Newark, NJ 07102

Professor E. Kröpl
Rensselaer Polytechnic Institute
Division of Engineering
Engineering Mechanics
Troy, NY 12181

Dr. Jack R. Vinson
University of Delaware
Department of Mechanical and Aerospace
Engineering and the Center for
Composite Materials
Newark, DE 19711

Dr. Dennis A. Nagy
Princeton University
School of Engineering and Applied Science
Department of Civil Engineering
Princeton, NJ 08540

Dr. J. Duffy
Brown University
Division of Engineering
Providence, RI 02912

Dr. J. L. Swedlow
Carnegie-Mellon University
Department of Mechanical Engineering
Pittsburgh, PA 15213

Dr. V. K. Varadan
Ohio State University Research Foundation
Department of Engineering Mechanics
Columbus, OH 43210

Universities (Con't.)

Dr. Ronald L. Huston
Department of Engineering Analysis
University of Cincinnati
Cincinnati, OH 45221

Professor G. E. M. Sih
Lehigh University
Institute of Fracture and
Solid Mechanics
Bethlehem, PA 18015

Professor Albert S. Kobayashi
University of Washington
Department of Mechanical Engineering
Seattle, WA 98105

Professor Daniel Frederick
Virginia Polytechnic Institute and
State University
Department of Engineering Mechanics
Blacksburg, VA 24061

Professor A. C. Eringen
Princeton University
Department of Aerospace and
Mechanical Sciences
Princeton, NJ 08540

Professor E. H. Lee
Stanford University
Division of Engineering Mechanics
Stanford, CA 94305

Professor Albert I. King
Wayne State University
Biomechanics Research Center
Detroit, MI 48202

Dr. V. K. Raghavan
Wayne State University
School of Medicine
Detroit, MI 48202

Dean B. A. Boley
Northwestern University
Department of Civil Engineering
Evanston, IL 60201

Professor P. G. Hodge, Jr.
University of Minnesota
Department of Aerospace Engineering
and Mechanics
Minneapolis, MN 55455

Dr. D. C. Drucker
University of Illinois
Dean of Engineering
Urbana, IL 61801

Professor N. M. Newmark
University of Illinois
Department of Civil Engineering
Urbana, IL 61803

Professor L. Bickson
University of California, San Diego
Department of Applied Mechanics
La Jolla, CA 92037

Professor William A. Nash
University of Massachusetts
Department of Mechanics and
Aerospace Engineering
Amherst, MA 01002

Professor G. Herrmann
Stanford University
Department of Applied Mechanics
Stanford, CA 94305

Professor J. B. Achenbach
Northwestern University
Department of Civil Engineering
Evanston, IL 60201

Professor S. B. Dong
University of California
Department of Mechanics
Los Angeles, CA 90024

Professor Burt Paul
University of Pennsylvania
Towne School of Civil and
Mechanical Engineering
Philadelphia, PA 19104

Universities (Con't.)

Dr. Z. Hashin
University of Pennsylvania
Department of Metallurgy and
Materials Science
College of Engineering and
Applied Science
Philadelphia, PA 19104

Dr. Jackson C. S. Yang
University of Maryland
Department of Mechanical Engineering
College Park, MD 20742

Professor T. Y. Chang
University of Akron
Department of Civil Engineering
Akron, OH 44325

Professor Charles W. Bert
University of Oklahoma
School of Aerospace, Mechanical,
and Nuclear Engineering
Norman, OK 73019

Professor Satya N. Atluri
Georgia Institute of Technology
School of Engineering Science and
Mechanics
Atlanta, GA 30332

Professor Graham F. Carey
University of Texas at Austin
Department of Aerospace Engineering
and Engineering Mechanics
Austin, TX 78712

Industry and Research Institutes

Dr. Jackson C. S. Yang
Advanced Technology and Research, Inc.
10006 Green Forest Drive
Adelphi, MD 20783

Dr. Norman Hobbs
Kaman Av/Dyne
Division of Kaman
Sciences Corp.
Burlington, MA 01803

Industry and Research Institutes (Con't.)

Argonne National Laboratory
Library Services Department
9700 South Cass Avenue
Argonne, IL 60440

Dr. M. C. Junger
Cambridge Acoustical Associates
1033 Massachusetts Avenue
Cambridge, MA 02138

Dr. V. Gdino
General Dynamics Corporation
Electric Boat Division
Groton, CT 06340

Dr. J. E. Greenspon
J. G. Engineering Research Associates
3831 Menlo Drive
Baltimore, MD 21215

Dr. K. C. Park
Lockheed Missile and Space Company
3251 Hanover Street
Palo Alto, CA 94304

Newport News Shipbuilding and
Dry Dock Company
Library
Newport News, VA 23607

Dr. W. F. Bozich
McDonnell Douglas Corporation
5301 Bolso Avenue
Huntington Beach, CA 92647

Dr. H. N. Abramson
Southwest Research Institute
8500 Culebra Road
San Antonio, TX 78284

Dr. R. C. DeHart
Southwest Research Institute
8500 Culebra Road
San Antonio, TX 78284

Dr. M. L. Baron
Weldinger Associates
110 East 59th Street
New York, NY 10022

Industry and Research Institutes (Con't.)

Dr. T. L. Geers
Lockheed Missiles and Space Company
3251 Hanover Street
Palo Alto, CA 94304

Mr. William Gaywood
Applied Physics Laboratory
Johns Hopkins Road
Laurel, MD 20810

Dr. Robert E. Nickell
Pacifica Technology
P.O. Box 148
Del Mar, CA 92014

Dr. M. F. Kanninen
Battelle Columbus Laboratories
505 King Avenue
Columbus, OH 43201

Dr. G. T. Hahn
Battelle Columbus Laboratories
505 King Avenue
Columbus, OH 43201

Dr. A. A. Hochrein
Dardalean Associates, Inc.
Springlake Research Center
15110 Frederick Road
Woodbine, MD 21797

Mr. Richard Y. Dow
National Academy of Sciences
2101 Constitution Avenue
Washington, DC 20418

Mr. H. L. Kington
Alresearch Manufacturing Company
of Arizona
P.O. Box 5217
111 South 34th Street
Phoenix, AZ 85010

Dr. M. H. Rice
Systems, Science, and Software
P.O. Box 1620
La Jolla, CA 92037

Unclassified

SECURITY CLASSIFICATION OF THIS PAGE (When Data Entered)

REPORT DOCUMENTATION PAGE		READ INSTRUCTIONS BEFORE COMPLETING FORM
1. REPORT NUMBER Technical Report No. 36 ✓	2. GOVT ACCESSION NO.	3. RECIPIENT'S CATALOG NUMBER
4. TITLE (and Subtitle) Influence of Dynamic Fracture Toughness on Dynamic Crack Propagation		5. TYPE OF REPORT & PERIOD COVERED Technical Report June '78 - Mar. '79
		6. PERFORMING ORG. REPORT NUMBER TN 36
7. AUTHOR(s) L. Hodulak, A.S. Kobayashi, A.F. Emery		8. CONTRACT OR GRANT NUMBER(s) N00014-76-C-0060 ✓
9. PERFORMING ORGANIZATION NAME AND ADDRESS Department of Mechanical Engineering, FU-10 University of Washington Seattle, Washington 98195		10. PROGRAM ELEMENT, PROJECT, TASK AREA & WORK UNIT NUMBERS WR 064-478
11. CONTROLLING OFFICE NAME AND ADDRESS Office of Naval Research Arlington, Virginia 22217		12. REPORT DATE March 1979
14. MONITORING AGENCY NAME & ADDRESS (if different from Controlling Office)		13. NUMBER OF PAGES 19
		15. SECURITY CLASS. (of this report) Unclassified
16. DISTRIBUTION STATEMENT (of this Report) Unlimited		15a. DECLASSIFICATION/DOWNGRADING SCHEDULE
17. DISTRIBUTION STATEMENT (of the abstract entered in Block 20, if different from Report)		
18. SUPPLEMENTARY NOTES		
19. KEY WORDS (Continue on reverse side if necessary and identify by block number) Dynamic fracture, fracture toughness, crack arrest, finite element analysis		
20. ABSTRACT (Continue on reverse side if necessary and identify by block number) A dynamic finite element code was used in its "propagation mode" to assess the differences in dynamic crack propagation in a wedge-loaded (WL) single-edged notch (SEN) specimen, a tapered double cantilever beam (TDCB) specimen and a rectangular double cantilever beam (RDCB) specimen. The dynamic fracture toughness, K_{ID} , versus the crack velocity, a , relations determined experimentally for WL-SEN, WL-TDCB and WL-RDCB specimens machined from Araldite B were used as dynamic fracture criteria and the resultant K_{ID} .		

DD FORM 1 JAN 73 1473

EDITION OF 1 NOV 65 IS OBSOLETE
S/N 0102-014-6601

UNCLASSIFIED

SECURITY CLASSIFICATION OF THIS PAGE (When Data Entered)

Unclassified

SECURITY CLASSIFICATION OF THIS PAGE(When Data Entered)

variations with crack propagations in the three specimens were compared with the corresponding experimental results. While the specific K_{ID} versus \bar{a} relations established for each specimen obviously yielded calculated K_{ID} which were in best agreement with the experimental K_{ID} for the respective specimen, the K_{ID} versus \bar{a} relations for the large WL-SEN specimen provided the best overall fit between the calculated and measured K_{ID} variations with crack propagation in all three specimens.

UNCLASSIFIED

SECURITY CLASSIFICATION OF THIS PAGE(When Data Entered)